J Comput Neurosci (2006) 20: 25–41
DOI 10.1007/s10827-006-4258-y

Membrane channel properties of premotor excitatory burst neurons may underlie saccade slowing after lesions of omnipause neurons

Kenichiro Miura · Lance M. Optican

Received: 25 March 2005 / Revised: 27 June 2005 / Accepted: 16 August 2005 / Published online: 20 February 2006

Abstract Chemical lesions of the brain stem region containing glycinergic omnipause neurons (OPNs) cause saccade slowing with no change in latency. To explore the mechanisms responsible for this deficit, simulation studies were performed with a conductance-based model of premotor excitatory burst neurons (EBNs) that incorporated multiple membrane channels, including the T-type calcium channel. The peak speed of a normal saccade was determined by the T- and NMDA currents in EBNs after the OPNs shut off. After OPN lesions, the model made slow saccades, because the EBN activity was lower than normal due to a reduced T-current (caused by the loss of hyperpolarization), and a reduced NMDA current (caused by a reduced glycine concentration around the receptors). Thus, we propose that two biophysical mechanisms are responsible for saccade slowing after OPN lesions: reduced T-current and reduced NMDA current, both of which are caused by the loss of glycine from OPNs.

Keywords Hodgkin-Huxley · eye movements · model · RIP · raphe interpositus nucleus · NMDA receptors · glycine · glutamate · saccades

Action Editor: Karen Sigvardt

K. Miura
Department of Integrative Brain Science, Graduate School of Medicine, Kyoto University,
Kyoto 606-8501, Japan

L. Optican (✉)
Laboratory of Sensorimotor Research, National Eye Institute, NIH,
Bethesda, MD 20892, USA
e-mail: LanceOptican@nih.gov

Introduction

Saccades are the fast eye movements that enable us to rapidly redirect our line of sight (Leigh and Zee, 1999). Many studies have been devoted to understanding the neural circuit that controls this class of eye movements (for a recent review, see Scudder et al., 2002). The premotor burst neurons for saccade generation (short or medium lead burst neurons, MLBNs) have been identified. MLBNs, which consist of both excitatory and inhibitory burst neurons (EBNs and IBNs), are distributed in the midbrain, pons and medulla (Hepp et al., 1989; Scudder et al., 2002; Sparks, 2002). For example, EBNs for horizontal saccades are in the pontine reticular formation, projecting to ipsilateral abducens nucleus, and IBNs for horizontal saccades are in the medullary reticular formation, projecting to contralateral abducens nucleus (Büttner-Ennever and Büttner, 1988; Hikosaka et al., 1980; Scudder et al., 1988; Strassman et al., 1986a; Strassman et al., 1986b). The activities of these MLBNs are closely related to the duration and velocity of saccades (Keller, 1974; Scudder et al., 1988; Strassman et al., 1986b; Van Gisbergen et al., 1981). Thus, it is believed that the ipsilateral EBNs provide the saccadic drive to the agonist muscle's final common pathway, and the ipsilateral IBNs inhibit the antagonist muscle's premotor neurons on the contralateral side. The contralateral EBNs are off throughout the saccade, because of inhibition from the ipsilateral IBNs. The contralateral IBNs fire a brief burst before saccade end, (Van Gisbergen et al., 1981) and may play a role in stopping the saccade (Quaia et al., 1999).

The system generating saccades also includes another class of brain stem neurons, referred to as *omnipause* neurons (OPNs), which are located in the pontine nucleus raphe interpositus, RIP (Büttner-Ennever et al., 1988). It has generally assumed that OPNs inhibit MLBNs, acting as *an inhibitory*

gate for the driving system of the saccades, based on the following observations. In awake animals, OPNs have tonic activity that ceases during saccades in any direction (Cohen and Henn, 1972; Keller, 1974; Luschei and Fuchs, 1972). Single unit recordings have also demonstrated that the pause of OPNs, caused by a hyperpolarization of their membrane potential, starts just before MLBNs begin firing (Keller, 1974; Yoshida et al., 1999). Anatomical findings demonstrated that OPNs project most densely to regions containing EBNs and IBNs (Langer and Kaneko, 1990; Strassman et al., 1987). Stimulation in the OPN region during saccades stops movements of the eyes immediately (Keller and Edelman, 1994).

Kaneko (1996) and Soetedjo et al. (2002) demonstrated that the peak velocity of saccades was decreased when the RIP, which contains the OPNs, is damaged. This phenomenon can not be explained if the only function of the OPNs is as an inhibitory gate system; they must also contribute, in some way, to the drive signal for saccade generation. The slow saccades suggest that the RIP lesion makes the firing rate of the EBNs smaller, which would result from a reduced outward membrane current in EBNs during saccades. Thus, this experimental finding gives a clue to the sources of the currents that form the activity of EBNs, which, in turn, determines the dynamics of saccades.

Previous physiological findings showed that there is a particular class of voltage-dependent calcium channels that activate at a low membrane potential (Huguenard, 1996, 1998; Perez-Reyes, 2003), referred to as "low-voltage-activated calcium channels" or, simply, T-type calcium channels. This class of channel mediates a transient calcium current, called the low-voltage-activated current, low-threshold calcium current or T-current, in response to a stepwise change in membrane potential from a hyperpolarized to a depolarized level (Huguenard, 1996, 1998; Perez-Reyes, 2003). Under physiological conditions, the T-current requires hyperpolarizing the membrane potential and subsequently allowing synaptic input to activate it (Koch, 1999). Experiments with the techniques of electrophysiology and molecular physiology have discovered detailed features of this class of channels (Perez-Reyes, 2003). Furthermore, in previous theoretical studies, the T-current in thalamic relay neurons (Huguenard and McCormick, 1992) and reticular neurons (Destexhe et al., 1994) has been quantitatively modeled. These discoveries motivated us to hypothesize that this current contributes to the activity of EBNs. Prior to saccade generation the MLBNs are inhibited by OPNs, and hence they would be hyperpolarized before saccades. The release from this inhibition, with subsequent synaptic inputs, would induce a significant amount of T-current. An inactivation of OPNs would result in the absence of this hyperpolarization of EBN membrane potential before saccades. At least, the membrane potential before saccades is higher when the OPNs are inactivated than when it is normal, leading to the prediction of a smaller T-current under OPN inactivation. Thus, this current may be a potential biophysical mechanism by which the saccades are accelerated if OPNs are intact, but slowed if OPNs are missing.

In a previous study (Miura and Optican, 2003), we constructed a detailed model of the saccade generator, including the MLBNs. In that model, the MLBNs were implemented as a nonlinear dynamical element, in which we assumed the existence of two phenomenological factors: post-inhibitory rebound depolarization (PIR) and a threshold for firing. With these two factors, the experimental findings from RIP lesion studies, i.e., saccade slowing without a change in latency, were successfully reproduced. Unfortunately, the modeling of the MLBNs in the previous study did not incorporate any biophysical mechanisms for producing the PIR or setting the threshold. Extending the model by incorporating details at the level of membrane currents would enable predictions of the effects of different receptor agonist and antagonist ligands. Thus, here we construct a conductance-based neuron model of MLBNs that incorporates the T-current, as well as standard synaptic channels that are commonly involved in any neuron models. This membrane model was used for the MLBNs in a simple, lumped saccade model to simulate the dependence of saccadic waveforms on membrane conductance changes. Through simulation studies of saccades generated with this model, we will show that the inclusion of a T-current can successfully reproduce the saccade slowing after OPN lesion/inactivation seen by Kaneko's group (Kaneko, 1996; Soetedjo et al., 2002). We also studied a possible contribution of NMDA receptors to saccade slowing after OPN inactivation. The neurotransmitter of OPNs is glycine (Horn et al., 1994), which has two major actions in synapses. First, it is inhibitory at strychnine-sensitive receptors, and second it is a positive neuromodulator, or co-agonist, at NMDA receptors (Johnson and Ascher, 1987; Thomson et al., 1989). Thus, the inactivation of OPNs may reduce the concentration of glycine around both types of receptors on EBNs. Reduction at the inhibitory receptor would reduce the hyperpolarization of the EBNs before saccades, and reduction at the NMDA co-agonist cite would reduce the glutamatergic saccadic drive on EBNs. Thus, the loss of the co-agonist could slow saccades by reducing the effectiveness of the normal saccade drive. We will show here the magnitude of this effect. Based on the present results, we will discuss the importance of the biophysical properties of MLBNs on the saccade slowing seen after OPN lesion/inactivation, as well as on the generation of saccades.

Methods

Model design

We used a conductance-based, single-compartment model of EBNs to examine the contributions of the biophysical properties of membrane channels to the generation of saccades before and after OPN lesion. We started with the Hodgkin-Huxley equations for modeling the action potential. Four other channels were added to model effects of excitatory and inhibitory inputs. A T-type calcium channel was added to model membrane rebound, a glycine channel to model OPN inhibition, and non-NMDA and NMDA channels to model excitatory inputs.

The conductance-based membrane model for EBNs

The equation used for describing the time evolution of the membrane potential of a neuron is:

$$C\frac{dV}{dt} = -I_L - I_T - I_{Na} - I_K - I_{Gly} - I_{Glu} \tag{1}$$

where V is the membrane potential of the EBN unit, C is the membrane capacitance (set to 1 $\mu F/\text{cm}^2$). I_L, I_T, I_{Na}, and I_K, denote the leak current, T-current, fast sodium current and delayed rectifier potassium current, respectively. I_{Gly} and I_{Glu} are synaptic currents mediated by glycinergic and glutamatergic synapses. (Note that inward currents have a positive sign.)

Leak current

The leak current is described in standard form as: $I_L = g_L(V - E_L)$, where g_L (= 0.4 mS/cm^2) and E_L (= −70 mV) denote the conductance and reversal potential of the leak current, respectively.

T-current

For this current, we adopted the model that was used by Destexhe et al. (1994). The current mediated by this channel, I_T, is described as follows:

$$I_T = g_T \cdot m^2 \cdot h \cdot (V - E_T) \tag{2}$$

$$\frac{dm}{dt} = -\frac{1}{\tau_m(V)}(m - m_\infty(V)) \tag{3}$$

$$\frac{dh}{dt} = -\frac{1}{\tau_h(V)}(h - h_\infty(V)) \tag{4}$$

$$m_\infty(V) = 1/(1 + \exp[-(V + 52)/7.4]) \tag{5}$$

$$h_\infty(V) = 1/(1 + \exp[(V + 80)/5]) \tag{6}$$

$$\tau_m(V) = 0.44 + 0.15/(\exp[(V + 27)/10]) + \exp[-(V + 102)/15]) \tag{7}$$

$$\tau_h(V) = 22.7 + 0.27/(\exp[(V + 48)/4]) + \exp[-(V + 407)/50]) \tag{8}$$

where g_T and E_T (= 120 mV) denote the maximal conductance and the reversal potential of this channel, respectively. The activation variable is m, and m_∞ and τ_m are its steady state value and its time constant, respectively. The inactivation variable is h, and h_∞ and τ_h are its steady state value and its time constant, respectively. The properties of this channel are summarized in Fig. 1A, B and C.

Fast sodium and potassium currents

The action potentials were modeled using Hodgkin-Huxley kinetics for the sodium current, I_{Na}, and the delayed rectifier current, I_K. It is well known that the EBNs produce a train of action potentials with unusually high frequency, i.e. over 1 kHz, during saccades. Here, to simulate action potentials of EBNs during saccades, we scaled the kinetics of the Hodgkin-Huxley model according to the modifications of Enderle and Engelken (1995). In addition, we chose a recent formalism for the kinetics of I_{Na} and I_K that was used in a model of hippocampal pyramidal cells by Traub et al. (1991). The equations for I_{Na} are as follows:

$$I_{Na} = g_{Na} \cdot m^2 \cdot h \cdot (V - E_{Na}) \tag{9}$$

$$\frac{dm}{dt} = \varphi \cdot (\alpha_m \cdot (1 - m) - \beta_m \cdot m) \tag{10}$$

$$\frac{dh}{dt} = \varphi \cdot (\alpha_h \cdot (1 - h) - \beta_h \cdot h) \tag{11}$$

$$\alpha_m(V) = \frac{0.32 \times (-46.9 - V)}{\exp[(-46.9 - V)/4] - 1} \tag{12}$$

$$\beta_m(V) = \frac{0.28 \times (V + 19.9)}{\exp[(V + 19.9)/5] - 1} \tag{13}$$

$$\alpha_h(V) = 0.128 \times \exp[(-43 - V)/18] \tag{14}$$

$$\beta_h(V) = \frac{4}{1 + \exp[(-20 - V)/5]} \tag{15}$$

where g_{Na} (= 120 mS/cm^2), E_{Na} (= 45 mV) and φ denote the maximal conductance, the reversal potential of this channel and a scaling constant, respectively; m and h are, respectively, activation and inactivation variables of the sodium channel.

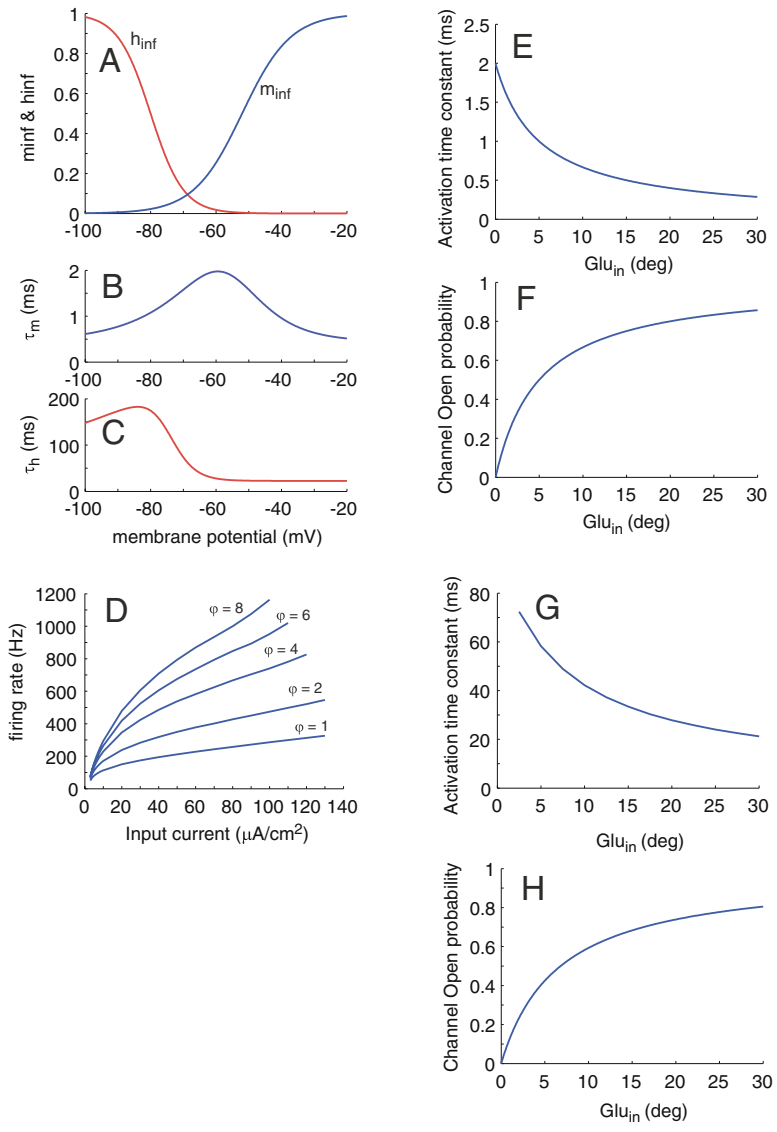

Fig. 1 Channel properties of the neuron model for EBN units. **A:** steady state properties of activation and inactivation variables (m and h) of T-channel. **B** and **C:** time constant as a function of membrane potential for the activation and inactivation variables of T-current. **D:** Relationships between the firing rate and the input current (F-I curves) for different gains are shown. **E** and **F:** the time constant of activation and channel open probability of non-NMDA channel as a function of $[Glu_{in}]$ at $\alpha_{nonNMDA} = 0.1$. G and H: the time constant of activation and channel open probability of NMDA channel as a function of $[Glu_{in}]$ at $\alpha_{NMDA0} = 0.05$.

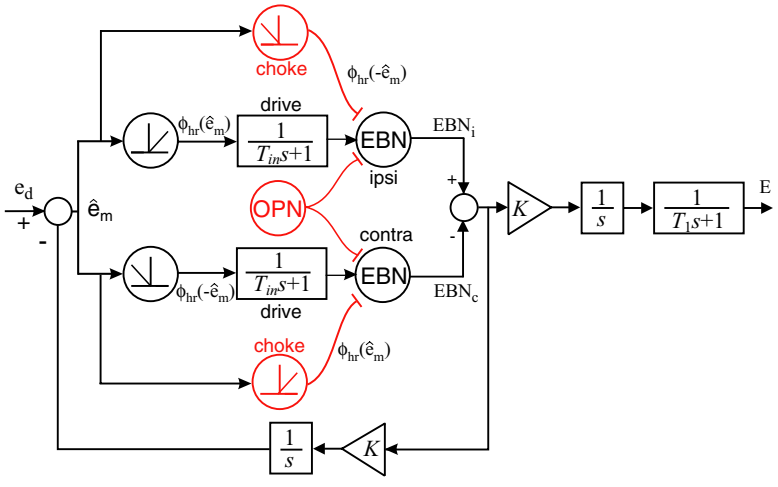

Fig. 2 A block diagram of the simulation system for the generation of saccades. To avoid clutter in the figure, details of the OPN unit are omitted. s denotes the Laplace variable. T_{in} denotes the time constant for the glutamate input to EBN unit. K is a constant. See text for these values. T_1 is set to 5 ms. Lines to EBNs with flat ending and with arrows indicate inputs to the glycine channel (i.e., inhibitory) and to the glutamate channels (i.e., excitatory), respectively. See text for more details.

$\alpha_m(V)$ and $\beta_m(V)$ are the voltage-dependent forward and backward rate variables for activation, and $\alpha_h(V)$ and $\beta_h(V)$ are those for inactivation. The equations for I_K are:

$$I_K = g_K \cdot n \cdot (V - E_K) \tag{16}$$

$$\frac{dn}{dt} = \varphi \cdot (\alpha_n \cdot (1 - n) - \beta_n \cdot n) \tag{17}$$

$$\alpha_n(V) = \frac{0.016 \times (-24.9 - V)}{\exp[(-24.9 - V)/5] - 1} \tag{18}$$

$$\beta_n(V) = 0.25 \times \exp[(-40 - V)/40] \tag{19}$$

where g_K (=10 mS/cm^2) and E_K (= −95 mV) denote the maximal conductance and the reversal potential of this channel, respectively, and n is the activation variable of the potassium channel. $\alpha_n(V)$ and $\beta_n(V)$ are the voltage-dependent forward and backward rate variables for activation. To fit the EBN firing rate, the kinetics of the sodium and potassium currents are multiplied by 8 (i.e., φ was set to 8), so that the model can generate action potentials at over 1 kHz. This implementation was necessary to examine the behaviors of the T-current during the high frequency oscillation of membrane potential during saccades (see also Discussion section). The relationships between firing rate of the neurons (F) and injected tonic current (I), i.e., F-I curves, generated by these equations are shown in Fig. 1D for reference.

Glycinergic current

It is known that inhibitory neurons that project to EBNs, i.e., OPNs and contralateral IBNs, use glycine as their neurotransmitter (Horn et al., 1994; Spencer et al., 1989). Therefore, our EBN model includes a glycinergic inhibitory synaptic channel. Previous studies have demonstrated that the glycine receptors act in a rapid manner when near body temperature. Specifically, a deactivation time constant in the range of 1.3–5.4 ms has been suggested (see discussion in Harty and Manis, 1998). The current, I_{Gly} is defined as follows:

$$I_{Gly} = g_{_{gly}} \cdot s \cdot (V - E_{Gly}) \tag{20}$$

$$\frac{ds}{dt} = \alpha_{gly} \cdot Gly_{in} \cdot (1 - s) - \frac{s}{\tau_{gly}} \tag{21}$$

where g_{Gly} (=1 mS/cm^2), E_{Gly} (= −80 mV) and s denote the maximal conductance, the reversal potential and the opening probability of this channel, respectively, and α_{gly} and τ_{gly} are constants. α_{gly} was set to 5.0, so that the inhibition by the OPN unit, whose design is described below, is immediate and opens more than 90% of the channels. τ_{gly} is the closing time constant of this channel, which was set to 2 ms in the simulations. (Note that changing the time constant from 1 to 5 ms did not change essential properties of saccade slowing after OPN inactivation.)

Glutamatergic currents

Although the excitatory neurotransmitter used in the neural circuit of the saccade generator is not known, it is reasonable to assume that it is glutamate, because the predominant fast excitatory neurotransmitter of the vertebrate central nervous system is glutamate (Koch, 1999). There are two major subclasses of glutamate channel receptors, a rapid type (non-NMDA receptors, e.g., AMPA receptors) and a slower type (NMDA receptors), which usually co-exist (McBain and Mayer, 1994). We incorporated both channel types in our model, hence I_{glu} is defined as $I_{nonNMDA}$+I_{NMDA}. The kinetics of $I_{nonNMDA}$ were essentially taken from the model of the AMPA receptor in Tegnér et al. (2002).

$$I_{nonNMDA} = g_{nonNMDA} \cdot s \cdot (V - E_{nonNMDA}) \tag{22}$$

$$\frac{ds}{dt} = \alpha_{nonNMDA} \cdot Glu_{in} \cdot (1 - s) - \frac{s}{\tau_{nonNMDA}} \tag{23}$$

where $g_{nonNMDA}$, $E_{nonNMDA}$ (=0 mV) and s denote the maximal conductance, the reversal potential and the opening probability of this channel, respectively; $\alpha_{nonNMDA}$ and $\tau_{nonNMDA}$ (= 2 ms, which is taken from Tegnér et al. (2002)) are the activation rate and time constant of deactivation, Glu_{in} is the drive input to the MLBNs from upstream, which is related to the motor error (in degrees, for details see below). The activation rate, $\alpha_{nonNMDA}$, was set to 0.1 ms^{-1}deg^{-1}. For reference, the activation time constant and channel opening probability in steady state as a function of Glu_{in} are shown in Fig. 1E and F, respectively.

The kinetics of I_{NMDA} were modified from Tegnér et al. (2002) with an added term describing the effect of glycine concentration around the receptor. The equations are as follows:

$$I_{NMDA} = g_{NMDA} \cdot s \cdot b_{Mg} \cdot b_{Gly} \cdot (V - E_{NMDA}) \tag{24}$$

$$\frac{ds_0}{dt} = \alpha_{NMDA0} \cdot Glu_{in} \cdot (1 - s_0) - \frac{s_0}{\tau_{NMDA0}} \tag{25}$$

$$\frac{ds}{dt} = \alpha_{NMDA} \cdot s_0 \cdot (1 - s) - \frac{s}{\tau_{NMDA}} \tag{26}$$

$$b_{Mg} = \frac{1}{1 + [Mg^{2+}]e^{-0.062 \cdot V}/3.57} \tag{27}$$

$$\frac{db_{Gly}}{dt} = \alpha_{GlyN} \cdot Gly_{NMDA} \cdot (1 - b_{Gly}) - \frac{b_{Gly}}{\tau_{GlyN}} \tag{28}$$

where g_{NMDA}, E_{NMDA} (=0 mV), s and s_0 denote the maximal conductance, the reversal potential, the channel opening probability and a synaptic variable proportional to the

neurotransmitter concentration of the NMDA channel, respectively. b_{Mg} represents the effect of the magnesium block, where we assumed that $[Mg^{2+}] = 1$ mM, as in Tegnér et al. (2002). We set the constants α_{NMDA0}, τ_{NMDA0}, α_{NMDA}, and τ_{NMDA} to 0.0015 $ms^{-1}deg^{-1}$, 2 ms, 0.5 and 100 ms, respectively. Except for α_{NMDA0}, the values were taken from Tegnér et al. (2002). We set the value of α_{NMDA0} by assuming the activation time constant was 30–40 times larger than that of the non-NMDA channel, so that NMDA channels had a relatively slower activation (Koch, 1999; McBain and Mayer, 1994). For reference, the activation time constant and channel opening probability at steady state as a function of Glu_{in} are shown in Fig. 1G and H, respectively. b_{Gly} is introduced here to represent the binding rate of glycine to the receptor.

Glycine is also a co-agonist at NMDA channels (Johnson and Ascher, 1987; Thomson et al., 1989). Here, we consider the effect of a variable amount of glycine (supplied by the OPNs) on NMDA channel currents. We modeled the time course of this factor with first order kinetics. The value of τ_{GlyN} was determined as 200 ms, which falls in a realistic range based on physiological findings (Johnson and Ascher, 1992) and a temperature correction (1 sec at room temperature, assuming Q_{10} of 2–3). α_{GlyN} was set to 0.01. Gly_{NMDA} was defined as the sum of a constant, the scaled output of OPNs (multiplied by 8.9), and the input from the inhibitory part of the feedback controller. In our main simulations, the constant was set to 0.1, and the output of OPNs was multiplied by 8.9, so that the binding rate of glycine is 0.17 when the OPN unit is inactivated and is 0.95 when it is normal. The choice of these values is uninformed by any behavioral or physiological data. Here, we assume a large difference in the binding rate of glycine associated with OPN conditions to see the possible contribution of NMDA channels to saccade slowing after OPN inactivation. To estimate the relative contribution of the reduced NMDA currents to saccade slowing after OPN inactivation, we also simulated saccades without an OPN contribution to the glycine concentration around the receptors, in which the constant was set to 9.0, achieving a constant glycine binding rate of 0.95 on its own.

The output from the neuron

The output from this neuron model is defined by $1/(1+\exp(-(V+15)))$, which acts as a threshold to convert the membrane voltage into a train of action potentials.

The simulation system for saccade generation

To simulate saccades with the conductance based neuron model of MLBNs, we prepared a simple lumped system for saccade generation. The primary purpose of this implementation was to examine whether the biophysical mechanisms incorporated in the neuron model could be responsible for the saccade slowing seen after OPN inactivation. The details of the closed-loop system around the EBNs are not of interest here. Therefore, we kept the saccade model as simple as possible.

Premotor circuit and feedback controller

The simulation system involves two EBNs. Here, the same neuron model above described is applied to both of them. A feedback controller provides the input to the EBNs based on the motor error. The EBN unit ipsilateral to the ongoing saccades receives a motor error related signal through the glutamatergic synapses, i.e., non-NMDA and NMDA channels. The feedback controller calculates a transformed motor error ϕ_{hr} ($\hat{e}_m$), where $\hat{e}_m$denotes the estimated motor error that is defined by the desired eye displacement (e_d) minus the estimated eye displacement (see below), ϕ_{hr} denotes a half-wave rectification function. Then the signal is fed to the EBN unit through a low pass filter (time constant of T_{in}). For the EBN unit contralateral to the ongoing saccades, the input is calculated in the same way as that for the ipsilateral EBN unit, but by replacing $\hat{e}_m$ with$-\hat{e}_m$. The feedback controller also provides an inhibitory signal (choke) to these EBNs through the glycine channel, which simulates a putative inhibitory input from the contralateral IBN. The inhibitory inputs are calculated based on the estimated motor error. For EBNs ipsilateral and contralateral to the ongoing saccades, the inputs are defined as ϕ_{hr} ($-\hat{e}_m$) and ϕ_{hr} ($\hat{e}_m$), respectively. One possible neural circuit that achieves this feedback control, and its justification, will be described in the Discussion section.

OPN unit

One OPN unit is included in this system, and it projects to both EBNs. The OPN unit is defined like those of classical models (Van Gisbergen et al., 1981). The state of the OPN unit is defined by the sum of a constant bias (= 1), a brief inhibitory trigger (20 ms inhibitory pulse = −2) starting at the same time the drive input reaches the EBNs, and an inhibitory latch signal. The magnitude of the latch signal is defined as the sum of outputs of left and right EBNs multiplied by 100, fed through a low pass filter (time constant 50 ms), so that the latch is effective if one of the two EBNs has a firing rate of at least 100 Hz. The state was rectified with the function ϕ_{hr} and then this signal was fed to the glycine channel on all EBNs. To simulate the RIP lesion/inactivation condition, the output of the OPN unit was always zero.

Downstream pathway

The downstream pathway from the premotor input, i.e., the neural integrator and extraocular muscles and tissues was

lumped together with a gain element (K) that determines the excursion of the eyes caused by one spike, an integrator and a low pass filter with an uncompensated time constant ($T_1 = 5$ ms). This is a reduced description of the downstream pathway in Van Gisbergen's model (Van Gisbergen et al., 1981), involving a pulse-step parallel pathway (one-zero system) to the oculomotor plant (two-pole system, with one of the poles being compensated by the zero in the pulse-step pathways). The signal sent to this structure is defined as $EBN_i(t) - EBN_c(t)$, the difference between the outputs of ipsilateral and contralateral EBNs. The same signal is fed back, temporally integrated and multiplied by K, to estimate the current displacement. This estimate of current displacement is used to calculate the estimate of dynamic motor error.

Preliminary simulations

The conductance values for the non-NMDA current ($g_{nonNMDA}$) and the T-current (g_T) in the neuron model, and the gain of the system (K), were adjusted so that the resulting saccades generated by the entire simulation system had peak velocities similar to those described in Soetedjo et al. (2002). The peak speed of saccades of ~10 deg amplitude was about 400 deg/s before, and 250 deg/s after, OPN inactivation. Note that the maximal conductance of the NMDA current only slightly affects the peak velocity for saccades of this size (see below for the details). The adjustment of these three constants was made by hand in a trial-and-error manner. The other constants, described above, were fixed. We now briefly describe the general effects of changing these values. The change in behavior of the proposed model is monotonic relative to an increase/decrease in these three constants. Generally, increasing g_T and $g_{nonNMDA}$ increases the firing rate of the EBN unit during ipsilateral saccades, making the simulated saccades faster. Increasing K also makes the simulated saccades faster, because this determines the amount of movement caused by one spike of the EBN unit. An increase in g_T increased the difference in peak velocity of simulated saccades before and after OPN inactivation. Choosing g_T of 1.2, $g_{nonNMDA}$ of 0.25 and K of 4.5 reproduced saccade slowing observed in the previous experimental studies. A similar reduction in peak velocity after OPN inactivation was achieved by increasing g_T and decreasing $g_{nonNMDA}$ (e.g., g_T of 1.3 and $g_{nonNMDA}$ of 0.2) without a reduced NMDA current. However, we used the former values in our main simulations (below), to explore the possible contribution of NMDA channels to saccade slowing after OPN inactivation.

In this study, we assumed that the input to EBNs is dependent on the dynamic motor error, which is a simplification of our previous models (Lefèvre et al., 1998; Optican and Quaia, 2002; Quaia et al., 1999). Although the actual temporal characteristics of the input to the EBNs are not known, we assume a first-order approximation (i.e., one time constant). The number of glutamate channels (non-NMDA and NMDA) on EBNs also affects the temporal characteristics of the synaptic current. Although these numbers are unknown, we assume that only their ratio is important. We regarded these two properties as parameters and examined whether the temporal characteristics have an effect on the activity of EBNs and resultant saccades before and after OPN inactivation. We used two parameters to adjust the temporal characteristics of the synaptic drive current during saccades, i.e., the time constant of the input to EBN units (T_{in}) and the maximal conductance of NMDA channel (g_{NMDA}). All simulations were performed with MATLAB and SIMULINK (The Mathworks, Natick, MA), running on a PC/AT compatible computer.

Results

First, we describe the properties of normal saccades, simulated using our simplified model, with the characteristics of EBN units described above. Second, simulated saccades during channel blockade will be shown to clarify the functional role of individual membrane channels in driving the saccades. Finally, we will show the results of saccade simulations under OPN inactivation conditions, which predict how the drive currents in the EBNs are modulated after the inactivation.

Normal saccades

Figure 3 shows an example of simulated normal saccades of 5, 10 and 20 deg. The spike counts (7, 13 and 26, respectively) for individual saccades are approximately linearly related to the saccade size (0.8 deg/spike). The peak velocity of the saccades increases in a non-linear manner (336, 412 and 476 deg/s, respectively). The peak firing rate of the EBN unit was 500, 584 and 654 Hz, respectively. The firing rate was defined as the reciprocal of the inter-spike interval (the time difference between two successive spikes, assigned to the time of the earlier spike). The peak firing rate was defined as the maximum firing rate after spline interpolation. The firing rate, which is directly related to eye velocity, increases as saccade size increases. The eye position data were smoothed with a digital two-pole Butterworth low-pass filter (cut-off frequency of 80 Hz) to get a robust estimate of peak velocity, which was defined as the maximum eye velocity computed from the smoothed eye position temporal profile.

To better understand the behaviors of the present model, the properties of the EBN unit ipsilateral to the ongoing saccade are summarized in Fig. 4. Figure 4A shows the membrane potential during a simulated saccade of 10 deg whose eye movement temporal profiles are shown in Fig. 3A and

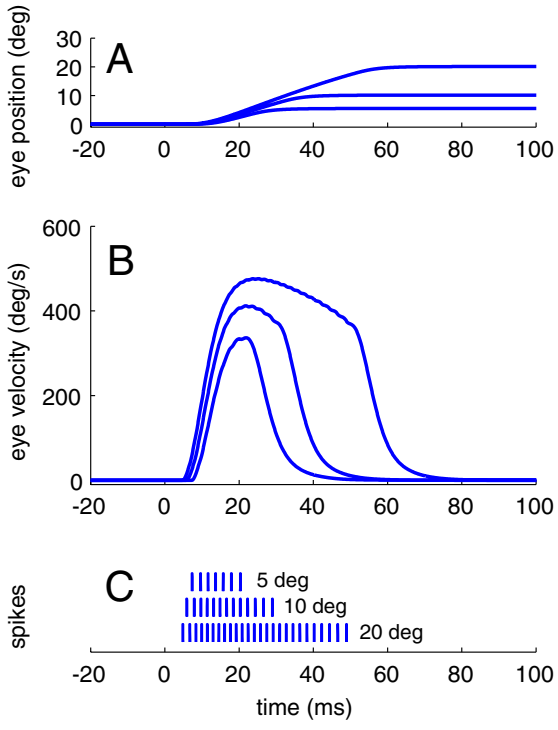

Fig. 3. Simulated normal saccades of 5, 10 and 20 deg. These saccades were simulated with the simulation system that has $g_T = 1.2$ (mS/cm^2), $g_{nonNMDA} = 0.25$ (mS/cm^2), $K = 4.5$ (dimensionless), $T_{in} = 5$ ms, $g_{NMDA} = 20\ g_{nonNMDA}$ (mS/cm^2). A: eye position temporal profiles. B: eye velocity temporal profiles. C: output of the EBN unit ipsilateral to saccades. The short bars indicate the time of an action potential (i.e., spike trains). Time zero means the onset time of the drive input to ipsilateral EBN.

B. While the OPN unit is active, the membrane potential stays at −77 mV because the glycine channel is open. At the instant of release from inhibition by the OPN unit, the drive input begins (time zero), the membrane of the ipsilateral EBN unit starts to depolarize and quickly reaches the threshold for action potential generation, followed by the generation of a spike. The feedback controller provides an excitatory input to the EBN unit through the glutamatergic synapses, until the motor error reaches zero, thus generating a train of action potentials. As the eyes reach the desired position, the feedback controller sends an inhibitory signal to the EBN unit through glycine channels (presumably from contralateral IBNs) to suppress the activation of the EBN unit ipsilateral to the ongoing saccade. At this time, both ipsilateral and contralateral EBNs become silent and the OPN unit is reactivated to keep all the EBN units silent. Note that the contralateral EBN unit was silent throughout the saccade.

In this example saccade, the total current in the ipsilateral EBN (Fig. 4B) is given by the sum of glutamatergic currents that consist of non-NMDA (Fig. 4E) and NMDA mediated (Fig. 4D) currents, and the T-current (Fig. 4C). As an aid to understanding the behaviors of individual channels, we show both raw traces after clipping the data during action

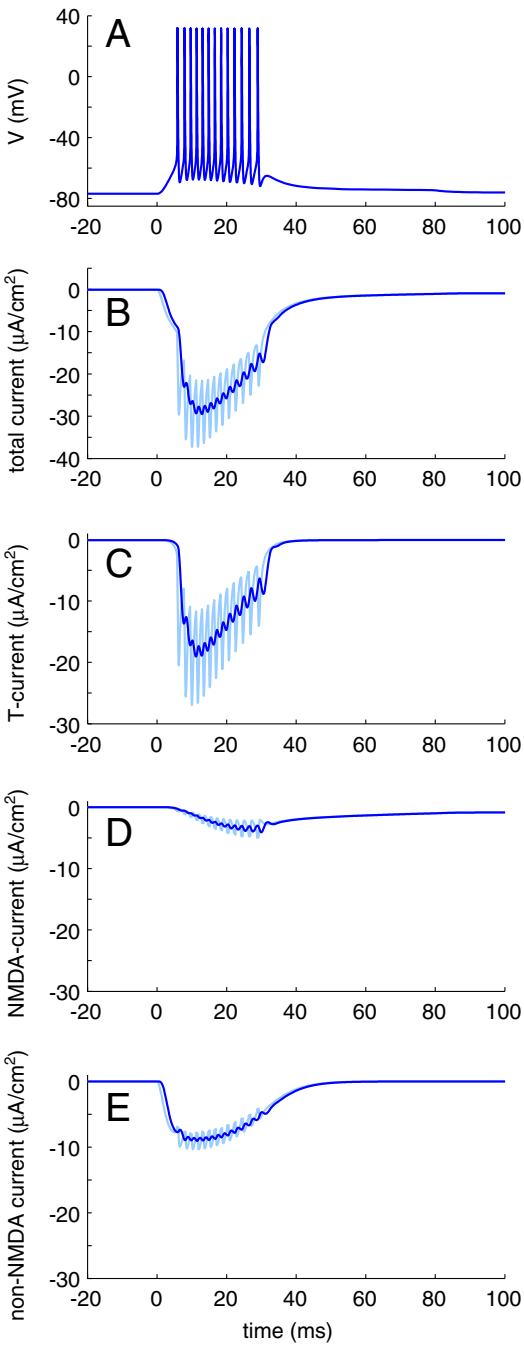

Fig. 4 Details of EBN unit during the saccade of 10 deg shown in Fig. 3. **A:** temporal profiles of membrane potential. **B:** Total outward current. **C:** T-current. **D:** NMDA mediated currents. **E:** non-NMDA mediated current. Light blue lines show raw traces after the removal of the data during action potentials. Blue lines show smoothed traces (see text for details). Time zero means the onset time of the drive input to ipsilateral EBN.

potentials (light blue lines) and smoothed traces (blue lines) after applying a digital three-pole Butterworth low-pass filter (cut-off frequency of 30 Hz). These low-pass filtered traces show the rough time course of the currents, as well as the conductance of individual channels. Roughly speaking, the

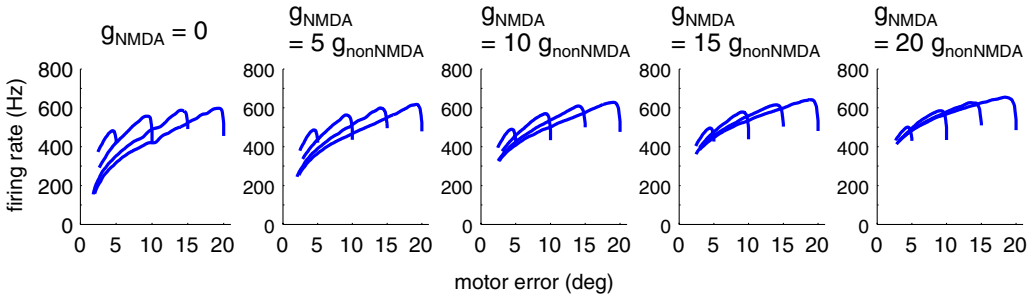

Fig. 5 The relationship between the instantaneous motor error and firing rate of ipsilateral EBN during saccades of 5, 10, 15 and 20 deg, for different synaptic drive currents (i.e., ratio of g_{NMDA} to $g_{nonNMDA}$). These saccades were simulated with the same parameters as Fig. 3.

non-NMDA channel acts as a low-pass filter with a short time constant (i.e., high cut-off frequency). The NMDA channel also acts as a low-pass filter, but with a much longer time constant than the non-NMDA channel (i.e., lower cut-off frequency). The T-channel acts as a high-pass filter that is less dependent on the motor error. Note that the NMDA channel has slower activation kinetics and is blocked by Mg^{2+} near or below the resting potential, resulting in a smaller contribution to the net driving signal even with its large maximal conductance. Thus, for a saccade of this size (∼10 deg), the non-NMDA current and T-current are the primary sources of activation of the ipsilateral EBN unit. The contributions of individual currents will be explained next.

Modifying temporal characteristics of the synaptic drive current changes the time course of the firing rate of the EBN unit ipsilateral to the ongoing saccades, and thus the temporal waveform of saccades. Importantly, we found that the temporal characteristics of the synaptic drive current significantly changed the relationship between the instantaneous motor error and the firing rate of the EBN unit ipsilateral to the ongoing saccades. Either an increase in T_{in} or g_{NMDA} changes this relationship. Note that the increase in T_{in} makes the synaptic drive current more sluggish. The increase in g_{NMDA} also makes the total glutamatergic input more sluggish, because of the slower kinetics of NMDA relative to non-NMDA channels. Thus, the increase in T_{in} and g_{NMDA} changes the temporal characteristics of the synaptic drive current in a similar way. Figure 5 shows examples of the relationship between the instantaneous motor error and the firing rate of the EBN unit for different values of g_{NMDA}. Each panel in Fig. 5 shows phase plots representing the relationships for saccades of 5, 10, 15 and 20 deg. Under $g_{NMDA} = 0$ (Fig. 5A, the extreme case), the phase plots obtained from saccades of different sizes were separate. The EBN unit showed a larger firing rate for smaller saccade sizes even at the same instantaneous motor error. Increasing g_{NMDA} decreases this separation of the phase plots for different sizes of saccades. In the rightmost panel ($g_{NMDA} = 20\ g_{nonNMDA}$), the phase plots for saccades of different sizes overlapped, which roughly corresponds to an invariant relationship between the firing rate and the instantaneous motor error. Note that "$g_{NMDA} = 20\ g_{nonNMDA}$" does not necessarily mean that the number of NMDA channel is twenty times larger than that of non-NMDA channel. It has been suggested that a single NMDA channel may have a much larger conductance than that of a single non-NMDA channel (Jahr and Stevens, 1987). Not surprisingly, a similar tendency in phase plots was seen when we changed T_{in} (not shown), because of a similar qualitative effect on the synaptic drive current. Van Gisbergen et al. (1981) examined the relationship between the instantaneous motor error and the firing rate of EBNs in monkeys. They reported that some EBNs showed separated phase plots for saccades of different sizes, similar to the simulation results in which g_{NMDA} and/or T_{in} are small. They also found that the majority of EBNs (more than 64%) had a roughly invariant relationship between the instantaneous motor error and firing rate, similar to the simulation results in which g_{NMDA} and/or T_{in} are large. One interpretation of these results is that different EBNs may have different densities of NMDA receptors, and that the EBNs with the densest NMDA receptors are the main mediators of the major part of the drive signal for saccade generation.

Selective blockade of channels

To better understand the properties of the drive current components on the model EBN unit during ipsilateral saccades, we examined the effects of selective blockades of different channels on the properties of saccades. The results of T-channel blockade, NMDA channel blockade and the blockades of both channels are summarized in Fig. 6. Generally, each blockade reduces the speed of saccades, because each removes the corresponding drive current component. However, because of the difference in temporal characteristics of these channels, the reduction of drive current, as well as of the speed of resultant saccades, is somewhat different in each case.

The selective blockade of the T-channel (simulated by setting $g_T = 0$, green lines) shows general reductions in the peak velocity of saccades. As described above, the T-channel acts as a high-pass filter. Therefore, the blockade of the T-channel reduces the early component of the

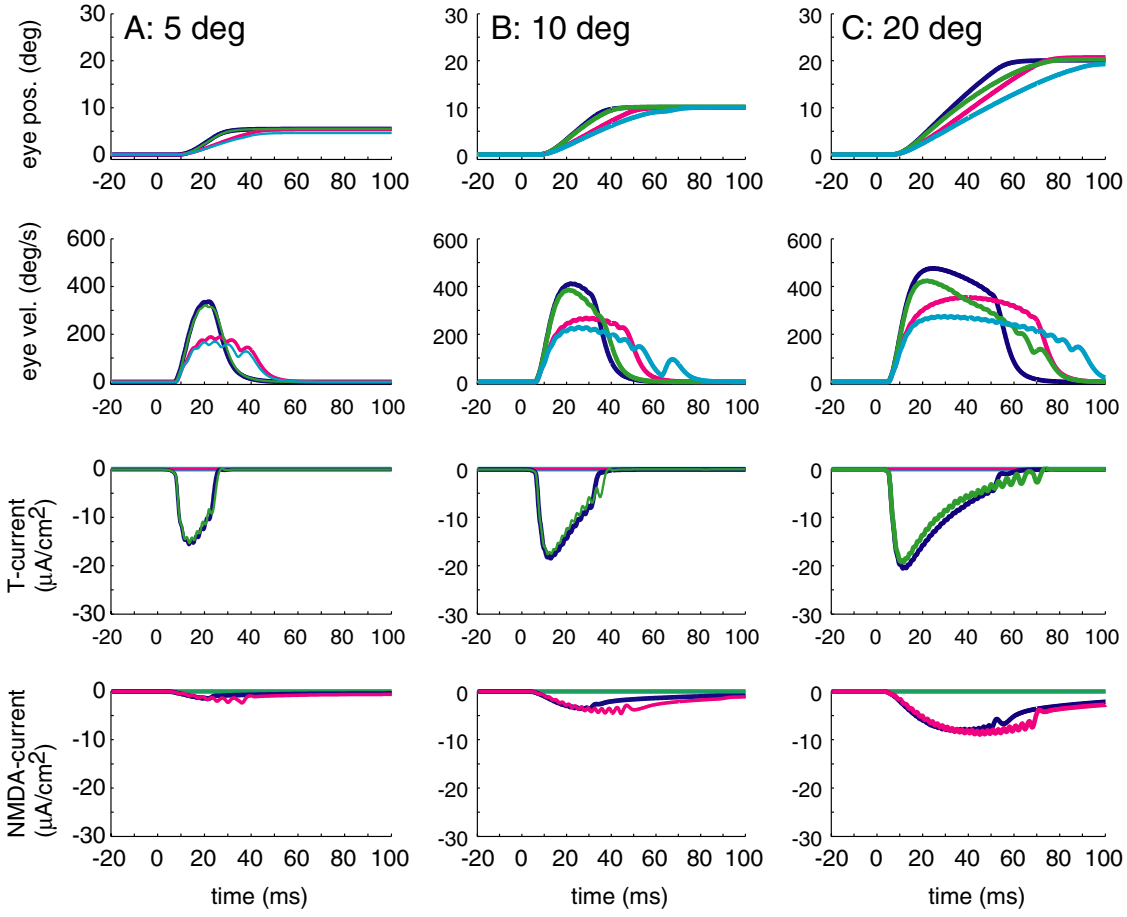

Fig. 6 Comparisons of saccades and properties of the model's ipsilateral EBN unit. Columns **A**, **B** and **C** are simulations for saccades of 5, 10 and 20 deg, respectively. Panels (top to bottom) are eye position, eye velocity, T-current, and NMDA-channel mediated current. In the panels for currents, we show smoothed traces obtained by applying a low-pass filter to the raw traces after clipping the data during action potentials. Blue lines indicate temporal profiles of saccades and properties of the ipsilateral EBN unit during normal saccades. Other traces are after the blockade of the T-channel (magenta lines), the NMDA channel (green lines) or both of these channels (cyan lines). (The current traces under the simultaneous blockade of T- and NMDA channels were always zero. Onset time of the drive input to the EBN unit is at time = zero. These saccades were generated by the system that has $g_{\mathrm{T}} = 0$ under the blocked condition or 1.2 (mS/cm^2) otherwise, $g_{nonNMDA} = 0.25$ (mS/cm^2), $K = 4.5$ (dimensionless), $T_{in} = 5$ ms, $g_{NMDA} = 0$ under the blocked condition or 20 $g_{nonNMDA}$ (mS/cm^2) otherwise.

drive current, resulting in a slower acceleration of initial eye movement.

The selective blockade of the NMDA channel (cyan lines) has a different effect from the blockade of the T-channel, as is easily predicted from the differences in temporal properties of these channels. A remarkable consequence of the selective blockade of NMDA channel is that the amount of decrease in peak velocity is dependent on the size of saccades. This is due to the slower activation kinetics of the NMDA channel. For saccades of 5 deg, the final eye position is reached before the NMDA channel is effectively opened. Therefore, the effect of the blockade of the NMDA channel on 5 deg saccades is fairly small. The effect of the blockade becomes more evident as saccades become larger because the duration of saccades becomes longer as saccade size increases. The reduction in saccade velocity caused by the selective blockade of the NMDA channel is seen well after the onset of saccades (say, 15–20 ms). The effect on the initial development of saccades is almost negligible, indicating that the initial part is dominated by non-NMDA and T- channel currents.

The simultaneous blockade of both channels (magenta lines) shows a general decrease in drive currents, as well as in saccade velocity. In this case, the drive current consists only of the current mediated by the non-NMDA channel, which acts as a low-pass filter with a small time constant (less than 2 ms for both the activation and deactivation phases).

Slow saccades after OPN inactivation

We have succeeded in adjusting the system parameters so that the present model can generate either normal saccades or saccades after OPN inactivation that are consistent with previous experimental findings. Figure 7 shows a comparison

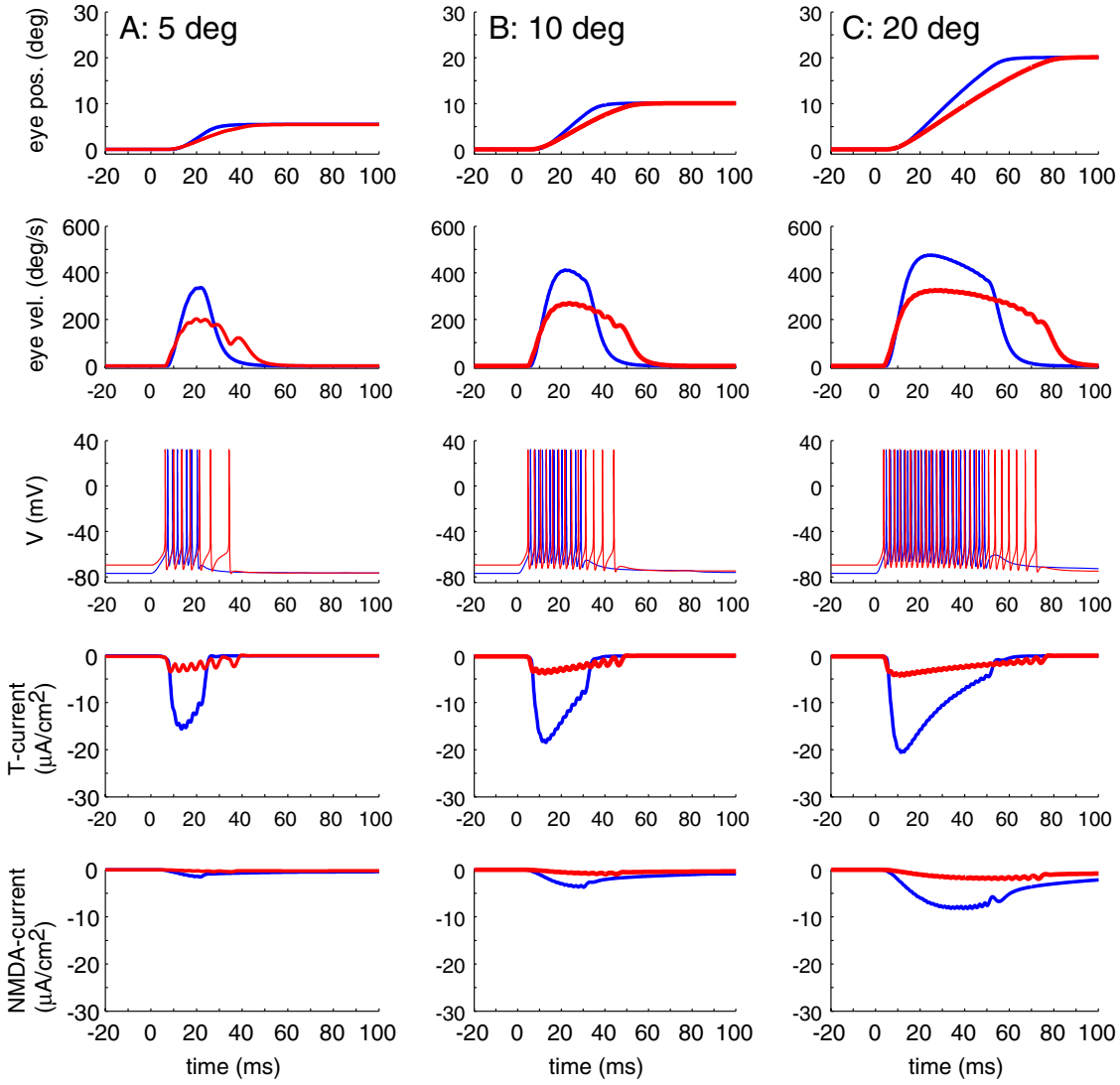

Fig. 7 Comparisons of simulated saccades and properties of the ipsilateral EBN unit before and after OPN inactivation. Red lines indicate temporal profiles of saccades and properties of the ipsilateral EBN unit after OPN Inactivation. Traces, top to bottom, are eye position, eye velocity, membrane potential, T-current, NMDA channel mediated current, respectively. Other conventions as in Fig. 6. These data were obtained from the system with $g_T = 1.2$ (mS/cm^2), $g_{nonNMDA} = 0.25$ (mS/cm^2), $K = 4.5$ (dimensionless), $T_{in} = 5$ ms, $g_{NMDA} = 20\ g_{nonNMDA}$ (mS/cm^2).

of eye velocity temporal profiles of saccades and properties of the EBN unit before and after OPN inactivation. This confirms that the peak velocity of saccades is slowed after OPN inactivation in saccades of any sizes. In saccades of 5, 10 and 20 deg/s, the peak velocity was reduced to 202, 270 and 326 deg/s when the OPN was inactivated (reductions of 134 (40%), 142 (34%) and 150 deg/s (32%) for saccades of 5, 10 and 20 deg, respectively). Note that the accuracy of saccades is essentially unaffected because the feedback controller is not disrupted by OPN inactivation. Therefore, the duration of saccades lengthens after OPN inactivation. Also, notice that the latency change was very small (less than 2 ms in this example), in accord with the data of Soetedjo et al. (2002)

Small differences have big consequences

As shown in the third row in Fig. 7, a noticeable difference in the membrane potential before saccades is seen after OPN lesions. When the OPN is normal, the membrane potential is hyperpolarized down to nearly −77 mV by the OPN inhibition, whereas it stays at about −70 mV (the resting potential of the leak current) when the OPN is inactivated. This difference in membrane potential, although small, is critical in the present model because it results in greatly different T-currents (temporal profiles are shown in the fourth row in Fig. 7). As shown in this panel, the T-current is generally four times larger (difference of about 15 μA/cm^2) when the OPN is normal than when it is inactivated. This difference can

be seen independent of the size of saccades. In the present model, this difference is the primary cause of reduction in the total drive current. The reduction in the total current, in turn, reduces the firing rate and, hence, results in slower saccades. Note that the saccade slowing in this model occurs because of a completely different mechanism from the cause of slowing in Scudder's model (Kaneko, 1989). As pointed out by Kaneko (1989), the Scudder model will make slow saccades after removing the OPNs because saccades start much too early, before the long-lead burst neurons can build up the drive signal. Data from Kaneko's study do not show such speed-dependent latency differences (Soetedjo et al., 2002). The mechanism of slowing after OPN inactivation in our new model, primarily by a reduced T-current (see below for another potential mechanism), is the first successful explanation of Kaneko's result. This property is almost independent of the temporal characteristics of the synaptic drive current we examined (not shown). Thus, our result leads us to hypothesize that a reduced T-current is one of the causes of the saccade slowing that follows OPN lesion/inactivation.

In these simulation results, we can see that there are differences in the currents mediated by the NMDA channel on the EBN unit before and after OPN inactivation (the bottom row in Fig. 7). This difference in the NMDA channel currents reflects the effect of a variable glycine concentration around the NMDA receptor, which results from the presence or absence of glycine from the OPN unit (see above). We have shown that the NMDA currents contribute more to the drive of saccades of larger sizes. In Fig. 7, remarkable differences can be seen in larger saccades (see e.g., the case of 20 deg saccade, rightmost column in Fig. 7). Thus, as easily predicted, the contribution of the reduced NMDA current to the net slowing of saccades depends on saccade size. We also examined saccade slowing after OPN inactivation without a contribution of OPNs to the glycine concentration (see Methods for details of simulations) to see the relative contribution of the reduced NMDA currents. Under this situation, the saccade slowing after OPN inactivation must be produced only by the reduced T-current, providing an estimate of its contribution. In saccades of 5, 10 and 20 deg/s, the reduced peak velocities were 122, 120 and 83 deg/s, respectively, in the case shown in Fig. 7. The contributions of the NMDA channel to saccade slowing were estimated as 9%, 23% and 45% for saccades of 5, 10 and 20 deg, respectively. Note that these saccades were simulated under the assumption that the contribution of OPNs to the glycine concentration around the receptor is also large. Thus, these estimates might be too large. Assuming a reduced effect of OPNs on the glycine concentration reduces the proportionate contribution of the NMDA channel. Unfortunately, there is currently no data to determine this contribution. However, this result establishes that a reduction in NMDA currents could significantly contribute to saccade slowing after OPN lesion, especially for larger saccades. Experimental tests of this prediction should enable the relative contribution of the two mechanisms *in vivo* to be determined.

Discussion

In this study, we constructed a conductance-based model of EBNs and simulated saccades using a simple lumped model with two EBN units. Extending our dynamic model (Miura and Optican, 2003) in this manner allowed us to incorporate detailed biophysical mechanisms that might underlie the generation of normal saccades, and cause saccade slowing after OPN inactivation. Here, we have demonstrated that the inclusion of the T-channel in the model of EBNs can reproduce the saccade slowing following OPN lesion/inactivation, because the T-current is reduced after OPN inactivation. Thus, we propose that the reduction in T-current may be one of the causes of saccade slowing seen after OPN lesion/inactivation. Furthermore, reduced glycine binding on the NMDA channel also causes a reduction of the drive current in the EBN unit. Based on this result, we propose that a reduced glycine concentration at the NMDA receptor may also contribute to the slowing of saccades after OPN inactivation.

Physiological realism

So far, no investigation has been performed of the details of the membrane properties of EBNs discussed here. In an attempt to maintain physiological and behavioral realism, all of the properties of the conductance-based model of EBNs used here were based on other models in the literature or on conservative assumptions. Here, we summarize some justifications of the EBN model and the entire simulation system for saccades.

The existence of EBN T-channels is a novel prediction from our present study, because it can explain the saccade slowing after OPN inactivation. Although the existence of this channel in EBNs has not been established, this channel is widely distributed in the brain and other organs (Perez-Reyes, 2003). Smith suggested the existence of this channel in vestibular nucleus neurons of the oculomotor system (Smith et al., 2002). The maximal conductance value (g_T) used in a previous theoretical study of thalamic neurons (represented by a single compartment model) was 1.75 mS/cm^2, based on experiments in thalamus (Destexhe et al., 1994). In this study, we used a value of 1.2 mS/cm^2 to make saccadic peak velocity appropriate before and after OPN inactivation.

The existence of depolarizing inputs to the EBNs has not been proven. Indeed, a scheme for saccade control has been proposed (Enderle, 2002) in which the EBNs do not need any excitatory input to generate saccades, because they are

assumed to be spontaneously active. However, physiological and anatomical evidence has shown direct and/or indirect projections from neurons in the SC, pons and the cerebellum to MLBNs (Chimoto et al., 1996; Keller et al., 2000; Noda et al., 1990). Thus, the most reasonable assumption is that EBNs receive excitatory inputs on glutamate channels, and in our model, the glutamate channels provide an external drive for normal saccades. After OPN inactivation the rebound depolarization is lost, but the glutamate channels provide enough drive to make slow saccades. In Enderle's model, inactivating OPNs would prevent saccades altogether because there are no external inputs to the EBNs' glutamate channels, and without OPNs our model shows that the T-current would be too small to elicit action potentials by itself.

Most neuron models include an inhibitory GABA channel, but no GABAergic neurons have been found that project to EBNs. However, it has been demonstrated that the neurotransmitter released by OPNs and horizontal IBNs is glycine (Horn et al., 1994; Spencer et al., 1989). Therefore, our model included the inhibitory fast chloride current of the glycine channel, but no GABA channel. However, vertical IBNs seem to release GABA, so EBNs in the vertical/torsional part of the saccadic system may depend upon GABA for inhibition.

The sodium and potassium channels were included to simulate action potentials, i.e., the high frequency oscillations of EBN membrane potential during saccades. The reason for the inclusion of these channels is that the mechanisms we would like to examine here are sensitive to membrane potential. Indeed, the kinetics of the T-channel are voltage dependent. Therefore, we needed to test the behavior of this channel during realistic changes in membrane potential. In this study, the kinetics of EBN action potentials was based on an existing model of hippocampal neurons, scaled to allow the higher firing rates of EBNs. The mechanism of action potential generation over 1 kHz still remains unclear. However, this issue is not our current concern. Notice that the choice of action potential dynamics itself did not influence our present conclusions. Even with the use of a leaky-integrate-and-fire model (not shown), we would reach the same conclusion.

To simulate eye movements and, more importantly, the environment around the EBNs during saccades, we constructed a simple lumped system for the generation of saccades. The final common pathway (the downstream structure from the EBNs) and the OPN unit were implemented in quite similar ways to the ones used in previous models (e.g., see van Gisbergen et al. (1981)). The feedback controller we used here has been used earlier, e.g., in the distributed model of saccade generation by Lefèvre et al. (1998). The important feature of their theory is that the cerebellum controls the flight of the eyes during saccades by using both an excitatory drive and an inhibitory choke signal. During saccades, the neurons in the contralateral fastigial nucleus, as well as in the contralateral SC, are active. Those neurons project to ipsilateral MLBNs, driving saccades. At (or near) the end of the saccade, the neurons in the ipsilateral fastigial nucleus are activated; their outputs are sent to contralateral IBNs to choke off the drive signal (from ipsilateral EBNs) at the motor neuron level (Optican, 2005; Optican and Quaia, 2002; Quaia et al., 1999). The connections from IBNs to contralateral EBNs needed by this scheme were shown by Strassmann et al. (1986b). The scheme in our simulation system is similar, except that the IBNs were not modeled explicitly; inhibition from the feedback loop simply caused the activity of the ipsilateral EBN to be clipped off at (or near) the end of saccades.

The primary purpose of this study was to examine potential biophysical properties that could contribute to drive saccades, and which could underlie saccade slowing after OPN lesion or inactivation. Therefore, many other details of the saccadic system are not within the scope of the present paper. However, even with the use of this simple system, the simulated saccades, both normal and after OPN inactivation, appear realistic.

As we have described earlier, there are no experimental results from biophysical studies of MLBNs. Examining properties of monkey EBNs with similar methods to those in previous studies would test the minimum requirements of our hypothesis, i.e., the existence of these ionic channels. Moreover, such experiments may provide quantitative details of conductance values for individual channels that would help to improve the model used here. The model also predicts (Fig. 6) that if a ligand that selectively blocked the T-type calcium channel (e.g., Huang et al. (2004)) were injected into the PPRF (Keller, 1974) horizontal saccades would become slower, even though OPNs were still active.

Comparisons with previous models

Almost all models of the saccadic system derive from Robinson's seminal model of the pulse-step generator (1973, 1975). In these classical models (Jürgens et al., 1981; Van Gisbergen et al., 1981; Zee et al., 1976; Zee and Robinson, 1979), the saccadic system is represented by a negative feedback control circuit based on an efference copy of eye displacement. Recent studies have focused on neuronal networks for motor control of saccades, based on discoveries of details of saccade-related neural activity in the brain stem (pons and superior colliculus: SC) and in the cerebellum (Arai et al., 1999; Dean, 1995; Lefèvre et al., 1998; Optican and Quaia, 2001; Quaia and Optican, 1997; Scudder, 1988). The functional roles of the cerebellum and/or the SC in saccadic control have been intensively studied (Arai et al., 1999; Dean, 1995; Lefèvre et al., 1998; Optican and Quaia, 2001; Quaia et al., 1999). Although there has been substantial progress in understanding the circuitry of the saccadic system, their neuronal elements (e.g., EBNs and OPNs) have

always been assumed to have only very simple properties, such as a single time constant (Lefèvre et al., 1998), a firing rate saturation (Arai et al., 1999; Dean, 1995), both a time constant and a saturation (Quaia and Optican, 1997) or simply a delay (Scudder, 1988). Thus, in the classical scheme only a simple role (e.g., as a high-gain amplifier) could be assigned to the EBNs. With such simplistic elements, it is not surprising that none of these models can explain the effects of OPN lesions found by Kaneko and colleagues(Kaneko, 1996; Soetedjo et al., 2002).

A simulation study by Kaneko (1989) showed that the Scudder model (see Scudder (1988) for details of this model) produced saccades that had decreased peak velocity and increased duration. However, this model predicts that the slower saccades after OPN lesions are a consequence of earlier triggering of the saccades. This early triggering is not consistent with the experimental findings from OPN lesion/inactivation studies, which consistently failed to find any systematic change in saccadic reaction time (see also discussion by Soetedjo et al. (2002)).

Enderle (Enderle, 2002; Enderle and Engelken, 1995) proposed a novel model of EBNs, using Hodgkin-Huxley equations modified to allow exogenous signals to control channel timing. In that model the EBNs are spontaneously active, and receive no signals from upstream (which is not physiologically realistic, see above). Instead, the spontaneous activity of EBNs is inhibited by OPNs before saccades and resumes after the OPNs cease firing. Enderle also introduced a post-inhibitory rebound property for the EBNs, by changing the effective time constants of sodium and potassium channels during the saccade (i.e., not according to the classical Hodgkin-Huxley equations). As a consequence, after release from inhibition by OPNs an initial bump in the firing rate was seen. Unfortunately, the relationship between an offset of the inhibitory input and the modified time constant of these channels is not part of the Hodgkin-Huxley equations, and was not discussed in his papers. Moreover, the EBNs were not incorporated into a complete system for generating saccades. Thus, the saccadic behaviors that might be produced by Enderle's EBN model before and after OPN lesion/inactivation are unknown.

In the previous study, we constructed a model of MLBNs as a computational element, in which we assumed the existence of two phenomenological factors: post-inhibitory rebound depolarization and a threshold for firing (Miura and Optican, 2003; Miura and Optican, 2006 (in press)). With these factors, all the major experimental findings from RIP lesion studies were successfully reproduced. The post-inhibitory rebound depolarization in this model provides an additional drive signal. Therefore, the removal of prior inhibition after OPN inactivation results in slower saccades because the additional drive is gone. In the current model, a similar function (i.e., an additional drive signal caused by the prior activation of OPNs) is achieved through the functions of the T-channel and of the NMDA channel. The release from prior inhibition by OPNs, with subsequent synaptic inputs given through glutamate channels, induces the flow of a significant amount of T-current, resulting in the rebound depolarization. Saccade slowing caused by a reduced NMDA current, our second mechanism, does not depend on the prior inhibition of the neurons, but on the glycine concentration around NMDA channels. The "threshold for firing" assumed in the previous model is naturally incorporated into the current conductance-based neuron model as the difference between the activation potential of spikes (about −58 mV, which is consistent with that of standard neurons) and the resting potential (about −70 mV, which is also realistic). This relationship, as in our previous model, prevents unrealistically early onset of saccades after OPN inactivation, which would be caused by the prelude activity of upstream LLBNs (not implemented here) if there were no threshold. Thus, the current model includes all the important functions of the previous computational version and gives more detailed predictions for the mechanisms that underlie saccade slowing after OPN lesion/inactivation. In contrast to Scudder's model (described above), neither our previous nor our current models require early triggering to generate slower saccades after OPN inactivation.

Potential mechanisms for saccade slowing

Here, we propose that the T-channel and NMDA channel may be responsible for the saccade slowing after OPN lesion/inactivation. For the T-current mechanism, the model predicts that the membrane potential of EBNs before saccades is more hyperpolarized when the OPN is normal than when it is inactivated. The NMDA mechanism predicts that, first, the glycine concentration around NMDA channels must be at sub-saturation level in the absence of OPNs. Second, the glycine concentration around the NMDA channels must be increased by the prior activity of OPNs. Finally, the conductance of NMDA channels should be large enough to contribute to saccade drive. Some physiological evidence suggests that the glycine concentration around NMDA receptors may be modulated, for example, by a spillover from nearby glycine receptors (Ahmadi et al., 2003). Thus, the first two NMDA predictions are not physiologically unrealistic. The third prediction could be tested by introducing a selective blocker for the NMDA receptor into the region of the EBNs (the PPRF).

Note that there may be other mechanisms contributing to saccade slowing after OPN lesion/inactivation not considered in this study. One such potential mechanism is the effect of glycine concentration on the amount of glutamate released at the pre-synaptic terminal (Turecek and Trussell, 2001). The amount of glutamate released is increased by an

increased glycine concentration around pre-synaptic terminals. If any change in the glycine concentration around the presynaptic terminal occurs after the OPN inactivation, the drive signal from the upstream structure of EBNs would also be modulated. However, their temporal characteristics have not been clarified yet, so this potential mechanism was not modeled here. Second, it is known that the OPNs project not only to regions containing EBNs but also to regions involving saccade-related neurons, such as the nucleus prepositus hypoglossi, the nucleus reticularis tegmenti pontis, the mesencephalic reticular nucleus, etc. (Langer and Kaneko, 1990). Thus, the effect of OPNs may not be restricted to EBNs. Furthermore, the OPNs may act as a neuromodulator in any of these sites through the effect of glycine concentration on NMDA synapses.

Functional significance of OPNs in the generation of saccades

This model hypothesizes not only the mechanisms of saccade slowing after OPN inactivation, but also the novel functional roles of the combination of OPNs and EBNs in generating saccades. Classically, the OPNs have been thought of simply as an inhibitory gate for saccades. However, this traditional interpretation may be insufficient if the properties of EBNs depend on membrane channels. Our results suggest some novel functions of the OPNs. First, the OPNs may add to, or facilitate, the saccade drive signal when their activity pauses. This mechanism is represented in our present model through the voltage dependence of the T-channel. Second, the OPNs may enhance the drive signal by raising the concentration of glycine around NMDA receptors on EBNs. In this context, the OPNs may act as a neuromodulator for the saccade burst generator. Thus, we propose that the combination of biophysical membrane properties of EBNs and the output of the OPNs play an important role in determining the size of the velocity command for saccades.

Both circuit and membrane properties govern behavior

In previous models of saccade control (Arai et al., 1999; Dean, 1995; Jürgens et al., 1981; Lefèvre et al., 1998; Optican and Quaia, 2001; Quaia and Optican, 1997; Robinson, 1975; Scudder, 1988; Van Gisbergen et al., 1981; Zee et al., 1976; Zee and Robinson, 1979) the properties of neural network circuits related to saccade generation have been the primary focus. Here, we have shown the possibility that the biophysical properties of EBNs, controlled by the activity of the OPNs, may also be important in determining saccadic dynamics (in this case, peak velocity and latency). The hypothetical mechanisms proposed here are based on assumptions about the membrane properties of EBNs, but the biophysical characteristics of EBNs have yet to be studied. New experiments, such as selective blockades of individual channels, or intracellular recordings, could test the feasibility of our hypotheses and would suggest ways to improve the current model, thus leading to a better understanding of the premotor structures of saccade generation.

References

Ahmadi S, Muth-Selbach U, Lauterbach A, Lipfert P, Neuhuber WL, Zeilhofer HU (2003) Facilitation of spinal NMDA receptor currents by spillover of synaptically released glycine. Science 300: 2094–2097.

Arai K, Das S, Keller EL, Aiyoshi E (1999) A distributed model of the saccade system: simulations of temporally perturbed saccades using position and velocity feedback. Neural. Networks 12: 1359–1375.

Büttner-Ennever JA, Büttner U (1988) The reticular formation. In: Büttner-Ennever JA, ed. Neuroanatomy of the Oculomotor System. Elsevier, Amsterdam, pp. 119–176.

Büttner-Ennever JA, Cohen B, Pause M, Fries W (1988) Raphe nucleus of the pons containing omnipause neurons of the oculomotor system in the monkey, and its homologue in man. J. Comp. Neurol. 267: 307–321.

Chimoto S, Iwamoto Y, Shimazu H, Yoshida K (1996) Monosynaptic activation of medium-lead burst neurons from the superior colliculus in the alert cat. J. Neurophysiol. 75: 2658–2661.

Cohen B, Henn V (1972) Unit activity in the pontine reticular formation associated with eye movements. Brain Res. 46: 403–410.

Dean P (1995) Modelling the role of the cerebellar fastigial nuclei in producing accurate saccades: The importance of burst timing. Neurosci. 68: 1059–1077.

Destexhe A, Contreras D, Sejnowski TJ, Steriade M (1994) A model of spindle rhythmicity in the isolated thalamic reticular nucleus. J. Neurophysiol. 72: 803–818.

Enderle JD (2002) Neural control of saccades. Prog. Brain Res. 140: 21–49.

Enderle JD, Engelken EJ (1995) Simulation of oculomotor post-inhibitory rebound burst firing using a Hodgkin-Huxley model of a neuron. Biomed. Sci. Instrum. 31: 53–58.

Harty TP, Manis PB (1998) Kinetic analysis of glycine receptor currents in ventral cochlear nucleus. J. Neurophysiol. 79: 1891–1901.

Hepp K, Henn V, Vilis T, Cohen B (1989) Brainstem regions related to saccade generation. In: Wurtz RH, Goldberg ME, eds. The Neurobiology of Saccadic Eye Movements, Reviews of Oculomotor Research, Vol. III. Elsevier, Amsterdam, pp. 105–212.

Hikosaka O, Igusa Y, Imai H (1980) Inhibitory connections of nystagmus-related reticular burst neurons with neurons in the abducens, prepositus hypoglossi and vestibular nuclei in the cat. Exp. Brain. Res. 39: 301–311.

Horn AK, Büttner-Ennever JA, Wahle P, Reichenberger I (1994) Neurotransmitter profile of saccadic omnipause neurons in nucleus raphe interpositus. J. Neurosci. 14: 2032–2046.

Huang L, Keyser BM, Tagmose TM, Hansen JB, Taylor JT, Zhuang H, Zhang M, Ragsdale DS, Li M (2004) NNC 55-0396 [(1S,2S)-2-(2-(N-[(3-benzimidazol-2-yl)propyl]-N-methylamino)ethyl)-6-fluoro-1,2,3,4-tetrahydro-1-isopropyl-2-naphtyl cyclopropanecarboxylate dihydrochloride]: a new selective inhibitor of T-type calcium channels. J. Pharmacol. Exp. Ther. 309: 193–199.

Huguenard JR (1996) Low-threshold calcium currents in central nervous system neurons. Annu. Rev. Physiol. 58: 329–348.

Huguenard JR (1998) Low-voltage-activated (T-type) calcium-channel genes identified. Trends Neurosci. 21: 451–452.
Huguenard JR, McCormick DA (1992) Simulation of the currents involved in rhythmic oscillations in thalamic relay neurons. J. Neurophysiol. 68: 1373–1383.
Jahr CE, Stevens CF (1987) Glutamate activates multiple single channel conductances in hippocampal neurons. Nature 325: 522–525.
Johnson JW, Ascher P (1987) Glycine potentiates the NMDA response in cultured mouse brain neurons. Nature 325: 529–531.
Johnson JW, Ascher P (1992) Equilibrium and kinetic study of glycine action on the N-methyl-D-aspartate receptor in cultured mouse brain neurons. J. Physiol. 455: 339–365.
Jürgens R, Becker W, Kornhuber HH (1981) Natural and drug-induced variations of velocity and duration of human saccadic eye movements: Evidence for a control of the neural pulse generator by local feedback. Biol. Cybern. 39: 87–96.
Kaneko CR (1989) Hypothetical explanation of selective saccadic palsy caused by pontine lesion. Neurology. 39: 994–995.
Kaneko CR (1996) Effect of ibotenic acid lesions of the omnipause neurons on saccadic eye movements in rhesus macaques. J. Neurophysiol. 75: 2229–2242.
Keller EL (1974) Participation of medial pontine reticular formation in eye movement generation in monkey. J. Neurophysiol. 37: 316–332.
Keller EL, Edelman JA (1994) Use of interrupted saccade paradigm to study spatial and temporal dynamics of saccadic burst cells in superior colliculus in monkey. J. Neurophysiol. 72: 2754–2770.
Keller EL, McPeek RM, Salz T (2000) Evidence against direct connections to PPRF EBNs from SC in the monkey. J. Neurophysiol. 84: 1303–1313.
Koch C (1999) Biophysics of Computation. Oxford University Press, Inc., New York, NY.
Langer TP, Kaneko CR (1990) Brainstem afferents to the oculomotor omnipause neurons in monkey. J. Comp. Neurol. 295: 413–427.
Lefèvre P, Quaia C, Optican LM (1998) Distributed model of control of sacades by superior colliculus and cerebellum. Neural. Networks 11: 1175–1190.
Leigh RJ, Zee DS (1999) The Neurology of Eye Movements. Oxford, New York.
Luschei ES, Fuchs AF (1972) Activity of brain stem neurons during eye movements of alert monkeys. J. Neurophysiol. 35: 445–461.
McBain CJ, Mayer ML (1994) N-methyl-D-aspartic acid receptor structure and function. Physiol. Rev. 74: 723–760.
Miura K, Optican LM (2003) Membrane properties of medium-lead burst neurons may contribute to dynamical properties of saccades. Proceedings of the 1st International IEEE EMBS Conference on Neural Engineering: 20–23.
Miura K, Optican LM (2006 in press) Saccade Slowing After Lesions of Omnipause Neurons Explained By Two Hypothetical Membrane Properties of Premotor Burst Neurons. In: Akay M, ed. Neural Engineering Brain Imaging And Brain-Computer Interface. John Wiley and Sons.
Noda H, Sugita S, Ikeda Y (1990) Afferent and efferent connections of the oculomotor region of the fastigial nucleus in the macaque monkey. J. Comp. Neurol. 302: 330–348.
Optican LM (2005) Sensorimotor transformation for visually guided saccades. Ann. NY Acad. Sci. 1039: 132–148.
Optican LM, Quaia C (2002) Distributed model of collicular and cerebellar function during saccades. Ann NY Acad. Sci. 956: 164–177.
Optican LM, Quaia Q (2001) From sensory space to motor commands: Lessons from saccades. Proc. IEEE EMBC Conf. 1: 820–823.
Perez-Reyes E (2003) Molecular physiology of low-voltage-activated t-type calcium channels. Physiol. Rev. 83: 117–161.
Quaia C, Lefèvre P, Optican LM (1999) Model of the control of saccades by superior colliculus and cerebellum. J. Neurophysiol. 82: 999–1018.
Quaia C, Optican LM (1997) Model with distributed vectorial premotor bursters accounts for the component stretching of oblique saccades. J. Neurophysiol. 78: 1120–1134.
Robinson DA (1973) Models of the saccadic eye movement control system. Kybernetik 14: 71–83.
Robinson DA (1975) Oculomotor control signals. In: Lennerstrand G, Bach-y-Rita P, eds. Basic Mechanisms of Ocular Motility and Their Clinical Implications. Pergamon Press, Oxford. pp. 337–374.
Scudder CA (1988) A new local feedback model of the saccadic burst generator. J. Neurophysiol. 59: 1455–1475.
Scudder CA, Fuchs AF, Langer TP (1988) Characteristics and functional identification of saccadic inhibitory burst neurons in the alert monkey. J. Neurophysiol. 59: 1430–1454.
Scudder CA, Kaneko CS, Fuchs AF (2002) The brainstem burst generator for saccadic eye movements: a modern synthesis. Exp. Brain. Res. 142: 439–462.
Smith MR, Nelson AB, Du Lac S (2002) Regulation of firing response gain by calcium-dependent mechanisms in vestibular nucleus neurons. J. Neurophysiol. 87: 2031–2042.
Soetedjo R, Kaneko CR, Fuchs AF (2002) Evidence that the superior colliculus participates in the feedback control of saccadic eye movements. J. Neurophysiol. 87: 679–695.
Sparks DL (2002) The brainstem control of saccadic eye movements. Nat. Rev. Neurosci. 3: 952–964.
Spencer RF, Wenthold RJ, Baker R (1989) Evidence for glycine as an inhibitory neurotransmitter of vestibular, reticular, and prepositus hypoglossi neurons that project to the cat abducens nucleus. J. Neurosci. 9: 2718–2736.
Strassman A, Evinger C, McCrea RA, Baker RG, Highstein SM (1987) Anatomy and physiology of intracellularly labelled omnipause neurons in the cat and squirrel monkey. Exp. Brain Res. 67: 436–440.
Strassman A, Highstein SM, McCrea RA (1986a) Anatomy and physiology of saccadic burst neurons in the alert squirrel monkey. I. Excitatory burst neurons. J. Comp. Neurol. 249: 337–357.
Strassman A, Highstein SM, McCrea RA (1986b) Anatomy and physiology of saccadic burst neurons in the alert squirrel monkey. II. Inhibitory burst neurons. J. Comp. Neurol. 249: 358–380.
Tegnér J, Compte A, Wang XJ (2002) The dynamical stability of reverberatory neural circuits. Biol. Cybern. 87: 471–481.
Thomson AM, Walker VE, Flynn DM (1989) Glycine enhances NMDA-receptor mediated synaptic potentials in neocortical slices. Nature 338: 422–424.
Traub RD, Wong RK, Miles R, Michelson H (1991) A model of a CA3 hippocampal pyramidal neuron incorporating voltage-clamp data on intrinsic conductances. J. Neurophysiol. 66: 635–650.
Turecek R, Trussell LO (2001) Presynaptic glycine receptors enhance transmitter release at a mammalian central synapse. Nature 411: 587–590.
Van Gisbergen JA, Robinson DA, Gielen S (1981) A quantitative analysis of generation of saccadic eye movements by burst neurons. J. Neurophysiol. 45: 417–442.
Yoshida K, Iwamoto Y, Chimoto S, Shimazu H (1999) Saccade-related inhibitory input to pontine omnipause neurons: an intracellular study in alert cats. J. Neurophysiol. 82: 1198–1208.

Zee DS, Optican LM, Cook JD, Robinson DA, Engel WK (1976) Slow saccades in spinocerebellar degeneration. Arch. Neurol. 33: 243–251.

Zee DS, Robinson DA (1979) A hypothetical explanation of saccadic oscillations. Ann. Neurol. 5: 405–414.